Land Surface Hydrology Parameterization over Heterogeneous Surface for the Study of Regional Mean Runoff Ratio with Its Simulations①

P4 A

Liu Jingmiao (刘晶淼)[1], Ding Yuguo (丁裕国)[2], Zhou Xiuji (周秀骥)[1] and Wang Jijun (王纪军)[2]

[1]Chinese Academy of Meteorological Sciences, Beijing 100081

[2]Nanjing Institute of Meteorology, Nanjing 210044

(Received January 5, 2001; revised September 21, 2001)

ABSTRACT

An analytical expression for subgrid-scale inhomogeneous runoff ratios generated by heterogeneous soil moisture content and climatic precipitation forcing is presented based on physical mechanisms for land surface hydrology and theory of statistical probability distribution. Thereby the commonly used mosaic parameterization of subgrid runoff ratio was integrated into a statistical-dynamic scheme with the bulk heterogeneity of a grid area included. Furthermore, a series of numerical experiments evaluating the reliability of the parameterization were conducted using the data generated by the emulated simulation method. All the experimental results demonstrate that the proposed scheme is feasible and practical.

Key words: Land surface process, Hydrology, Subgrid scale, Heterogeneous distribution, Probability distribution density

1. Introduction

Land surface hydrology is a key link in the land surface process model (LSPM). In reality, runoff, infiltrability and evapotranspiration associated with rainstorms or intense rainfall events are not distributed evenly at any regional scale (Zhang, 1987; Zhang and Ma, 1992; Ding, 1994; Zhang and Li, 1998). Hence, the inhomogeneity of the landsurface hydrological fluxes and their description remain one of the unsolved frontier problems hitherto in the context of LSPMs (Avissar, 1992; Giorgi, 1997). Theoretically, land surface hydrology is an innegligible link of land-atmosphere hydrological cycle. In the framework of runoff theories of Dunne and Horton (refer to Pielke, 1990 and Zhou, 1997) the runoff is strongly and nonlinearly dependent upon atmospheric rainfall forcing and hydraulic properties of land surface or soils. On one hand, the spatial / temporal heterogeneities of precipitation provide similar mechanisms of water sources for runoff generation. On the other hand, stochastic and complicated physical properties of surface and status are undoubtedly responsible for heterogeneous distribution of runoff. It has been recognized by the meteorological community (Dikinson et al., 1986; Seller et al., 1986; Warrilow et al., 1986; Xue et al., 1991; Avissar, 1992, 1993; Giorgi, 1997) that the interactions of these processes lead to random complexity of a land surface hydrological process.

①This work is supported jointly by the Major-Subject Program of the National Natural Science Foundation of China (Grant No.49899270) and the National Key Basic Research of China (G1998040911).

Science the precision of averaged regional runoff is adversely affected by the inhomegeneous distribution of precipitation and soil moisture, those big–leaf–type models suffer from the basic assumption that grid area is uniformly covered by one kind of vegetation (Dikinson et al., 1986). The typical example of such models are BATS (Biosphere– Atmosphere Transfer Scheme) and SiB / SSiB models (Sellers et al., 1986; Xue et al., 1991), although these models offer relatively elaborated biological description.

Because the inhomogeneous distribution of related atmospheric and surface parameters, e.g., precipitation and soil moisture, adversely affect the calculation precision of regional averaged runoff, it is evidently inadequate if only the homogeneity assumption of a big–leaf–type model is met.

Surface heterogeneities at any scale(Avissar, 1992, 1993; Giorgi, 1997) result essentially from the interactions among diversity of the ecosystem, intricate terrain, spatial variability of soil properties, human activities and inhomogeneous distribution of regional precipitation. Generally, such inhomogeneities exist at any scales. In GCM models, for instance, rainfall is calculated based on a coupled atmospheric condensation and moist convective scheme, leading to an actually assumed homogeneous distribution of precipitation falling onto a grid area with the consequence of a general underestimate of instantaneous rainfall intensity inside, which is unrealistic because a precipitating system or storm only covers a fraction of the grid area with different rainfall intensities at different grid.

To overcome these weaknesses, two particular probability density functions (PDF) are applied to describe the horizontal distribution of precipitation and regional soil water content respectively for grid scale surface in the present study. For this study we assume that the actual precipitation area constitute only a part of the entire grid box and the horizontal distribution within the grid can be approximately denoted as a particular probability density function (PDF) at any time step, applies as a method equally to the study of horizontal distributions of regional soil water content and other surface parameters.

As for area–averaged fluxes over a heterogeneous surface, the Mosaic method is used in computing the fluxes of momentum, moisture and heat in the subgrid regions. Obviously this method evidently means that a large quantity of calculations has to be performed (and thus costly) and the ensuing objective effective synthesis of those mean fluxes is not so easy. Fortunately, in recent years a promising (Avissar, 1992; Giorgi, 1997) "statistical–dynamic" technique has been developed for land surface process parameterization. The present work will mainly improve analytic expressions of inhomogeneous runoff ratio with which to resolve the intricate mechanism of a surface hydrological event into integral expressions for flux contributions of top–layer soil water saturation and unsaturation in the subgrid area. It is theoretically demonstrated that the grid mean runoff ratio calculating can be simplified into these fluxes weighting over subgrid dissimilar surfaces or soil properties.

2. Heterogeneous runoff and dimensionless runoff ratios

According to Horton and Dunne (refer to Pielke, 1990 and Zhou, 1997), surface runoff normally consists of two events: 1) runoff production due to the excess of precipitation intensity P over soil infiltrability f (i.e.,$P > f$) in the case of unsaturated soil (soil water saturation $S < 1$), 2) runoff production due to the occurrence of precipitation over saturated or supersaturated surfaces ($S \geqslant 1$) and impermeable surface. In the second case all precipitation P turning into runoff (Entekhabi and Eagleson, 1989; Avissar, 1993). The corresponding runoff expression is given as

$$r = \{P - f | P > f,\ S < 1\} \bigcup \{P | S > 1\} \ . \tag{1}$$

Although not all related variables are entirely independent of each other, for a short time (e.g., a few minutes or more) it is likely to approximately assume S and P to be independent at the point where the effect of previous soil moisture is not included.

With this assumption, runoff ratio $E(r)/k$ at any unit time–step may be written as

$$\frac{E(r)}{k} = \int_0^1 \int_f^\infty (P - f) f_P(P) f_S(S) dP dS + \int_1^\infty \int_0^\infty P f_P(P) f_S(S) dS dP \ , \tag{2}$$

where $f_P(P)$ and $f_S(S)$ denote the PDF of precipitation intensity and relatively effective saturation of soil moisture respectively, and k is the fraction of the grid area affected by precipitation. This k has been studied theoretically and observationally (Eagleson 1984; Eagleson and Wang 1985; Eagleson et al., 1987). Assuming that over fraction k of the GCM grid area, the mean runoff ratio is $E(P)/k$ (Warrilow et al., 1986), the probability of precipitation intensity P, is exponentially distributed as the following form:

$$f_P(P) = \frac{k}{E(P)} \exp\left[- k \frac{P}{E(P)} \right] \ . \tag{3}$$

where $E(P)$ is the expectation of precipitation over the entire grid area. The regional mean of actual precipitation strength expressed by $E(P)/k = E^*(P)$, Eq.(3) may be rewritten as

$$f_p(p) = \frac{1}{E^*(p)} \exp\left[- \frac{P}{E^*(P)} \right] \ . \tag{4}$$

The negative exponent pattern of spatial distribution density for the PDF of precipitation has been confirmed (Warrilow et al., 1986; Zhang, 1987; Zhang and Ma, 1992: Ding, 1994; Zhang and Li, 1998). Ding (1994) has also demonstrated from the statistical–physical perspective that at grid points, the temporal frequencies of rainfall is probably gamma distributed. So the gamma distribution is applied to spatial and temporal rainfall distributions.

As mentioned earlier, the runoff event is not only closely related to the horizontal distribution of rainfall but also to surface or soil hydraulic properties with comprehensive factor represented by soil wetness. Therefore, in the surface layer, effective relative soil saturation defined by $S = \theta / \theta_{sat} = \theta / n$, where θ is the active volumetric soil moisture content and θ_{sat} is the saturation magnitude (equivalent to effective soil porosity n). As a first–order approximation a two–parameter gamma PDF (Avissar, 1993) as follows is applied to describe the heterogeneity of surface soil water content

$$f_S(S) = \frac{\lambda^\alpha}{\Gamma(\alpha)} S^{\alpha - 1} \exp(-\lambda S) \qquad \lambda,\ \alpha > 0 \quad S \geqslant 0 \ , \tag{5}$$

where α and λ denote the shape and scale parameter of PDF respectively.

Normally, soil infiltrability depends on soil moisture content and the vertical infiltration, mainly on the gradients of the capillary and gravity forces (Warrilow et al., 1986; Zhou, 1997). So some empirical expressions are applied to describe single–point infiltration (Zhou, 1997). Mathematically, the depiction of infiltration remains unsolved. To address this problem, applying the expression of vertical water potential in porous media, which agree with physical interpretation and Darcy's law, to moisture yields:

$$q = L(S)\left(\frac{\partial \psi}{\partial Z} + 1 \right) \ , \tag{6}$$

where $L(S)$ is the unsaturated hydraulic conductivity of the soil at relative soil saturation S and ψ is the matric potential. When the top–layer soil interface is saturated due to abundant precipitation or foreign origin followed by vertical infiltration, the top–later infiltration has the form

$$f = L_1\left[\left.\frac{\partial\psi}{\partial S}\right|_{S=1}\frac{\partial S}{\partial Z}+1\right], \tag{7}$$

with (7), the saturation and the vertical infiltration almost (slightly affected by soil texture structure) take place synchronously.

The approximate form of (7) is

$$f \approx L_1\left[\left.\frac{\Delta\psi}{\Delta S}\right|_{S=1}\frac{\Delta S}{\Delta Z}+1\right]. \tag{8}$$

where L_1 is the hydraulic conductivity of saturated surface–layer soil evidently. If only the top–layer soil is taken into account, then the infiltration expression can be given empirically by

$$f = L_1 + L_1 v(1-S), \tag{9}$$

where $v = \left(\left.\frac{\Delta\psi}{\Delta S}\right|_{S=1}\frac{1}{\Delta Z}\right)$ is the S–relative change rate of water potential for top–layer saturation. (9) indicats that the infiltration f hinges on the soil moisture S, top–layer hydraulic conductivity L_1 and also v. Given constant L_1 and v at $S \ll 1$, f will be bigger. In this case f is dependent on capillary, gravity hydraulic conductivity as well as soil physical properties and its texture. With soil moisture close to saturation, i.e., $S \to 1$, f approaches L_1, implying that the minimum f is only associated with soil physical properties and texture.

Substituting (3), (5) and (9) into (2) an appropriate integration yields

$$\frac{E(r)}{k} = \frac{E(P)}{k}\frac{\lambda^{\alpha}}{\Gamma(\alpha)}\int_0^1 S^{\alpha-1} e^{-kf/E(P)-\alpha S/E(S)}\,dS + \frac{E(P)}{k}\left[1-\frac{r(\alpha,\lambda)}{\Gamma(\alpha)}\right]. \tag{10}$$

where $\gamma(*,*)$ denotes an incomplete Gamma function, and $\Gamma(\alpha)$ is a complete one. Introducing the dimensionless runoff ratio R

$$R = \frac{E(r)}{E(P)}, \tag{11}$$

a further integration of (10) gives

$$R = \frac{e^{-H_1}}{\left(1-\frac{H}{\lambda}\right)^{\alpha}\Gamma(\alpha)}\gamma\left[\alpha,\ \lambda\left(1-\frac{H}{\lambda}\right)\right]+\left[1-\frac{\gamma(\alpha,\lambda)}{\Gamma(\alpha)}\right]. \tag{12}$$

where

$$H = \frac{kL_1 v}{E(P)} = \frac{L_1 v}{E^{*}(P)}. \tag{13}$$

$$H_1 = L_1 v + H. \tag{14}$$

$$\lambda = \frac{\alpha}{E(S)}, \tag{15}$$

and

$$E'(P)=\frac{E(P)}{k} . \tag{16}$$

(12) shows that the runoff ratio R is usually dependent upon two possible factors as given below:

(1) The second term on the right hand side (*rhs*) of (12) $1-\gamma(\alpha, \alpha/E(S))/\Gamma(\alpha)$ indicates that with less infiltrated or a saturated fraction ($S \to 1$), all precipitation is transformed into runoff. Mathematically, $\gamma(\alpha, \alpha/E(S))/\Gamma(\alpha) \leqslant 1$ suggests runoff genesis, irrespective of the magnitudes of $E(S)$ and α.

(2) The first term on the *rhs* of Eq.(12) $e^{-H_1}/[(1-H/\lambda)^{\alpha}\Gamma(\alpha)]\gamma(\alpha, \lambda(1-H/\lambda))$ shows that with $S \ll 1$, runoff occurs only under the condition of $P > f$. (16) reveals that when $E(S)$ is unchanged, the bigger the shape parameter α, the bigger the scale parameter λ. Given the mean rainfall intensity $E(P)$ and constants v, L_1 and k, $E(S)$ depends on the order of magnitude of α and S.

The shape parameter α is expressed by the statistical theory (Tian, 1991) as

$$\alpha=\frac{E^2(S)}{\sigma^2}=\left(\frac{1}{C_v}\right)^2 . \tag{17}$$

where C_v is a variation coefficient. As a result, the spatial variability of S (soil moisture content) influences runoff greatly. Especially when S–relative water potential change rate equals zero ($v \to 0$), Eq.(12) becomes

$$R=\frac{\gamma\left(\alpha, \frac{\alpha}{E(S)}\right)}{\Gamma(\alpha)}+1-\frac{\gamma\left(\alpha, \frac{\alpha}{E(S)}\right)}{\Gamma(\alpha)}=1 . \tag{18}$$

$R=1$ means that all rainfall becomes runoff under the condition that the surface is impermeable or supersaturated.

3. The reliability of the runoff scheme

In the present study, the rainfall event in the Henan Province on July 6–9, 1999 is investigated in order to test the reliability of the runoff scheme presented above. The result shows that from 0000–2300 BT (Beijing time) July 7, the rainfall frequency distribution is of natural negative exponents (Fig. 1).

No theoretical proof has been developed to concern the spatial pattern of the relative soil moisture saturation S, but S in Eq.(1) is mathematically equivalent to the volumetric weight of the moisture (Olkin et al., 1980) W_s, that is

$$S \approx W_s = d_p W , \tag{19}$$

where W is the volumetric weight of total soil, $d_p (= \rho_p / \rho_w)$ is the relative density of soil particles, ρ_w is moisture soil density, ρ_p is dry soil density. Since there exists a linear relationship between W and the real thermal inertia (RTI) (Tian, 1991; Xiao et al., 1994; Yu and Tian, 1997; Ma, 1998) and a nearly linear relationship between W and the apparent thermal inertia (ATI), considering the relation between S and W_s in (19), therefore S can be written as a function of RTI or ATI

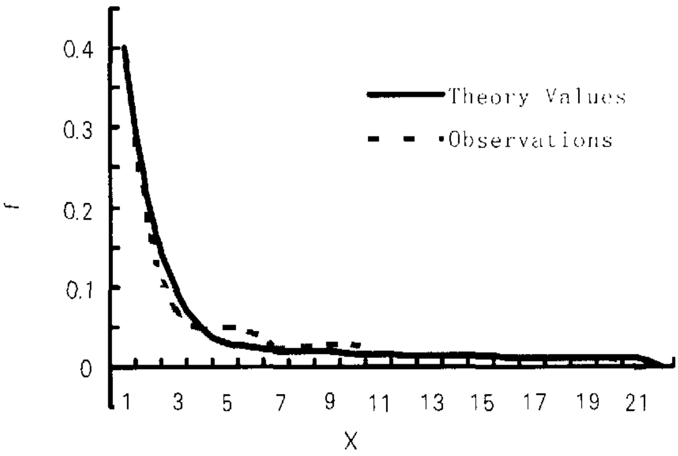

Fig. 1. 24-hr rainfall frequency distribution (with the abscissa scaled by 5(x − 1) mm), 7th July, 1999 in Henan Province.

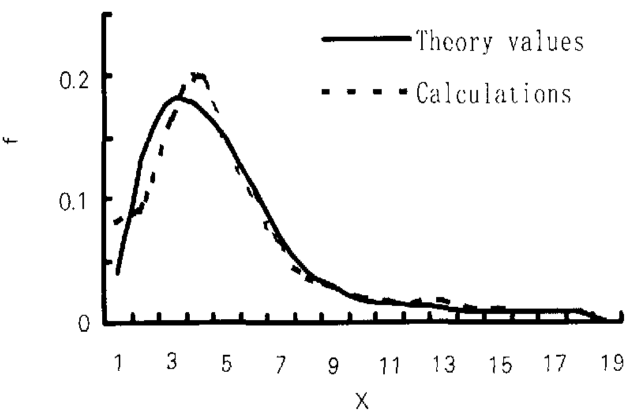

Fig. 2. ATI frequency distribution on September 13, 1999 with the abscissa scaled by (x − 96)%

$$S_w = a + b(\mathrm{ATI}) \tag{20}$$

$$S_u = a + b(\mathrm{RTI}) \ . \tag{21}$$

Some authors have indicated that the relationship can be expressed approximately as a power function (Tian, 1991; Xiao et al., 1994; Yu and Tian et al., 1997), but it is demonstrated that the parameters involved in the relation (as in Eq.(21)) are linked in a linear form, that is, when the RTI has a Gamma distribution (with distribution parameters a and λ), the S_u also has the Gamma distribution, and the following parameters are related as

$$\lambda' = \lambda / b \,, \tag{22}$$

$$\alpha' = \alpha \,. \tag{23}$$

Based on (20) or (21), the soil moisture S can be indirectly derived through the corresponding RTI or ATI.

The NOAA satellite data from September 13, 1999 was used to derived the ATI for the Yangtze delta sector, and the ATI frequency distribution and its density curve are shown in Fig. 2a with the distribution parameters of α= 5.9 and λ= 1.67. The agreement between the calculated and observed distributions is at exceedingly high confidence level, in full conformity to a Gamma distribution. The frequency distribution of soil moisture derived from the ATI is almost the same as what of the analog of Fig. 2 (figure omitted). Observation practice shows that the soil moisture with steady infiltration at any time intervals normally maintains a Gamma pattern. Greater details about this will be given in a separate paper. All these provide sufficient observational evidence for our theoretical research.

4. Experiments on the feasibility and sensitivity of the parameterization scheme

4.1 *Experiments on the feasibility*

A simple numerical simulation was done to demonstrate the physical implication of the parameterization scheme proposed. Fig. 3 shows variations of R as a function of soil moisture saturation $E(S)$ over unsaturated loam and sand fractions. It is seen that with a small α (for example, α= 1), the runoff ratio R decreases dramatically with the increase of $E(S)$, particularly when $E(S)$> 0.2; but for a larger α (for example, α= 5), the contribution of $E(S)$ to R reduces slowly versus growing $E(S)$. Inspection of Figs. 2a and 2b indicates that although the order of magnitude of R in unsaturated loam belt is bigger than that of in sand belts, the variation are the same in both loam and sand belts. These results indicate that heterogeneous distribution of soil moisture (e.g., the distribution shape of parameter α) influence the strength of grid mean runoff directly.

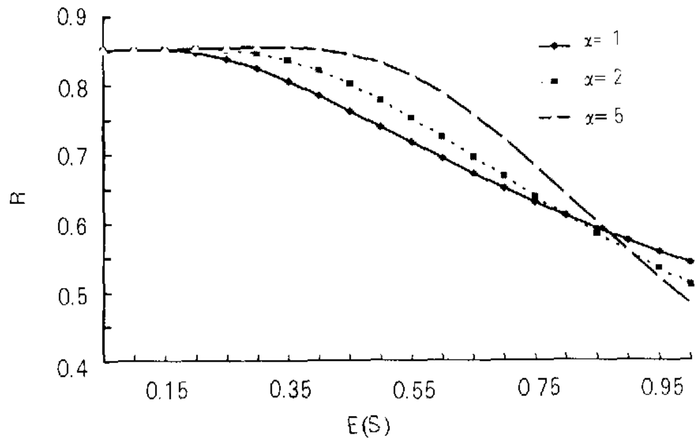

Fig. 3a. $E(S)$-dependent contribution of an unsaturated loam area to R.

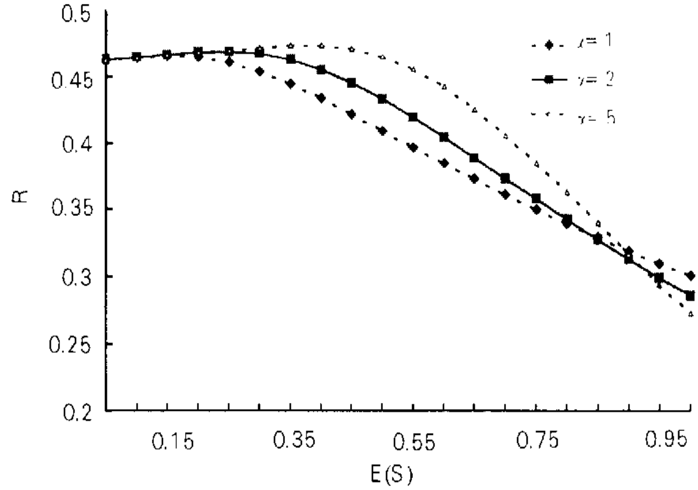

Fig. 3b. The same as Fig. 3a but for in sand band.

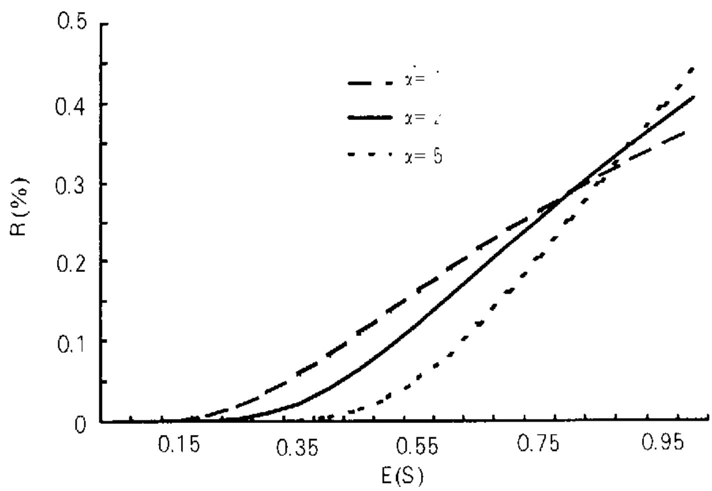

Fig. 4. $E(S)$-varying contribution of moisture-saturated sands to runoff ratio R.

The contribution of the saturated sandy fraction to R is studied with R as a function of $E(S)$ at different α (α= 1,2,5) (Fig. 4). Figures 4 shows that in saturated area, the increase of R with the increase of $E(S)$ becomes faster with smaller α. With α= 5, $E(S)$'s contribution to R slows down with increase of $E(S)$. This indicates that in a unsaturated area (i.e., a small α), the contribution of $E(S)$ to R remains limited, while in a saturated area, the contribution of $E(S)$ to R is considerable. Comparison also shows that the high $E(S)$ means greater wetness of soil, having bigger contribution to runoff, regardless of the magnitude of α. This also suggests that the mechanism for the generation of local runoff is associated with distributed rainfall intensity. Since the Horton-type (Dunne-type) runoff production occurs largely

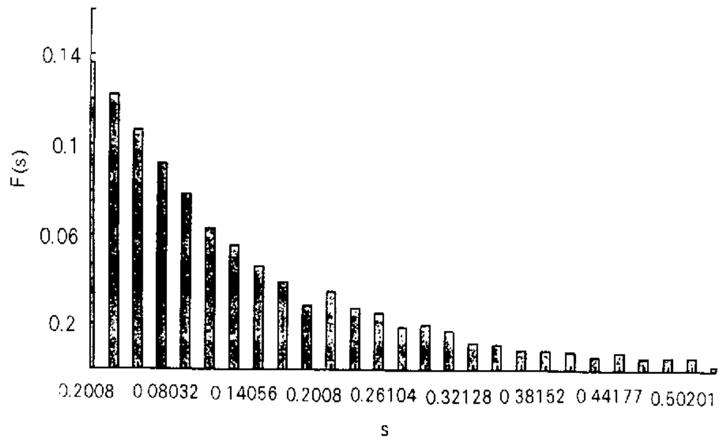

Fig. 5. Frequency histogram of soil moisture saturation indices S.

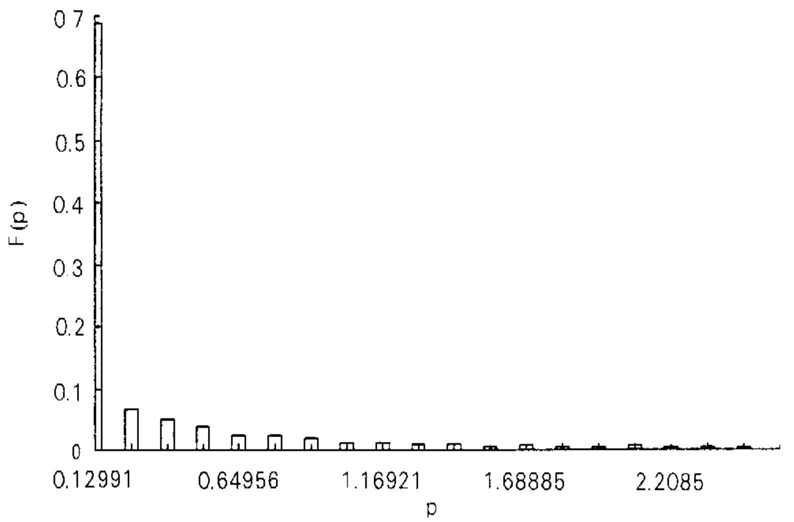

Fig 6. The same as Fig. 5 except for precipitation P.

in a saturated (unsaturated) belt, the heterogeneously distributed precipitation intensity (P) has a critical effect on the regional mean runoff ratio R. Figures 3 and 4 respectively present the two components of regional mean runoff ratio R, that is the first and second rhs terms in (12).

This study shows that for the distribution of soil moisture, a small $E(S)$ indicates a drier condition of the whole grid region and, consequently, most of runoff is produced actually through water exfiltration in an unsaturated belt (the Dunne component). Since saturated area is rather small and not necessarily the region experiencing the highest rainfall intensity, the saturation-related runoff makes less contribution to the total runoff in the whole concerned area.

A higher $E(S)$ suggests greater wetness observed in the grid on the whole and, irrespective of the value of α, the saturation–generated runoff makes relatively greater contribution, in contrast to the slightly reduced share from the unsaturation–produced counterpart. Moreover, the experiment on the relation of unsaturation runoff ratio and the precipitation parameter k (figure not shown) reveals that small area with high rainfall strength leads to smaller contribution to runoff production.

Generally, the conditions of soil moisture in saturated and unsaturated belts are steadyly adjusted by instantaneous distribution of atmospheric precipitation, the surface runoff is crucially associated with inhomogeneities of rainfall intensity and soil water distributions.

4.2 *Sensitivity experiment*

To conduct sensitivity experiments on area mean runoff over a heterogereous region, a stochastic technique is adopted in numerical calculation (Larsen and Pense, 1982; Allen et al., 1975; Ding and Zhang, 1989). The procedure is as follows:

(1) The dimensionless runoff ratio is evaluated with (12) (refer to columns 8 in Tables 1 and 2). The samples of S and P (S and P follow Gamma and negative–exponent distribution respectively) are randomly put onto subgrid points for computing runoff ratio by mosaic scheme (refer to columns 9 in Tables 1 and 2), then the difference of calculations by the proposed scheme and the mosaic scheme is examined. The experiment is repeated to produce error expectation: $E|R - R^*| < \varepsilon$, where ε is the critical error.

(2) Variations of the R are investigated as a function of $E(S)$ and $E(P)$ with different values of k and α (Tables 1 and 2).

(3) The Clapp–Hornberger scheme for hydraulic models (Clapp and Hornberger, 1978) is applied with given parameters L_1, ψ_s, b and v for different types of soil (Table 3). Figures 5 and 6 show the frequency histograms of soil moisture saturation (S) and precipitation (P) with respective space distribution parameters.

Table 1 shows that given the rainfall parameters $k \approx 0.33$, $E(P) \approx 0.48$ and the soil water spatial distribution parameters $\alpha = 3.80623$ and $\lambda = 14.7243$, the theoretical value of R is 0.9133 and subgrid points averaging R^* is 0.8467, with a relative error of 7.172% averaged over five runs for the runoff ratios on clay loam land.

Table 1. Runoff ratios obtained from stochastic experiments (the parameters slightly changed)**

Code	Rainfall		Soil water		Runoff		Runoff ratio		
	k	$E(P)$	α	λ	α	λ	TV	SA	RE(%)
001	0.33490	0.4912	3.83828	14.7937	0.3871	0.9304	0.9137	0.8472	7.278
002	0.33080	0.4722	3.78238	14.6722	0.3630	0.9102	0.9128	0.8447	7.461
003	0.34260	0.4743	3.78281	14.6733	0.3671	0.9171	0.9119	0.8441	6.908
004	0.34230	0.4982	3.82091	14.7592	0.3948	0.9334	0.9134	0.8488	7.072
005	0.32930	0.4968	3.80676	14.7232	0.3861	0.9229	0.9142	0.8489	7.143
Average	0.33598	0.4865	3.80623	14.7243	0.3796	0.9228	0.9132	0.8467	7.172

** TV = theoretical value; SA = subgrid average; RE = relative error (%).

Table 2. The same as Table 1 but for more markedly changed parameters**

Code	Rainfall		Soil water		Runoff		Runoff ratio		
	k	$E(P)$	α	λ	α	λ	TV	SA	RE(%)
001	0.33170	0.4968	1.94315	10.6259	0.3823	0.9215	0.9114	0.8350	8.291
002	0.50200	0.9750	3.74438	14.5908	0.8306	0.9443	0.9204	0.9022	1.977
003	0.43300	0.7454	2.80391	12.5272	0.6027	0.9225	0.9166	0.8764	4.386
004	0.38760	0.6036	3.25709	13.5220	0.4945	0.9531	0.9146	0.8595	6.024
005	0.38310	0.3610	3.55818	12.0013	0.2784	0.9513	0.8957	0.8106	9.501
Average	0.40748	0.6364	3.06134	12.6534	0.5177	0.9385	0.9117	0.8567	6.036

** TV – theoretical value; SA – subgrid average, RE – relative error (%).

Table 3. Values of L_1, b, t and ψ_s (cm) (saturation water potential) taken from Pielke (1990) for different types of soil

Soil type	L_1 (cm/s)	ψ_s (cm)	b	ψ
Sand	0.01760	−12.1	4.05	49.005
Siltyclay loam	0.00017	−35.6	7.75	276.256
Loam	0.00070	−47.8	5.39	275.642
Clay loam	0.00025	−63.0	8.51	257.642
Clay	0.00013	−40.5	0.482	19.521

Table 2 shows that with remarkably changed parameters k, $E(P)$, α and λ, the mean relative error is about 6.0%, the maximum relative error below 10% and the minimum around 2% (the last column) from five out of more than 30 runs performed. This suggests that the area mean (R) obtained by the theoretical expressions differs very little from that obtained by the mosaic scheme, regardless of the change of parameters. Thereby, the theoretical runoff ratio that is expressed by (12) is reliable and feasible.

Furthermore, numerical experiments for runoff ratios with each of the 12 kinds of soil land lead to the following conclusions.

(1) As a function of the area average rainfall strength $E(P)$, the maximum of related ratio R is associated with clay soil, and minimum of R with sandy clay soil when $E(P)$ is fixed. And all ratios display slow rise for any of the soil types with the increase of $E(P)$ (Fig. 7).

(2) The mean runoff from mosaic calculation is more sensitive to the change of precipitation parameter k than that from analytical expressions (12). With a smaller k, the mosaic scheme gives great relative error related to the analytic expression (figure not shown).

(3) Since it is on a regional scale, different kinds of soil generate different values of R with the maximum (minimum) from clay (sand) land, the runoff ratio R increases with $E(S)$ under the condition of rainfall intensity fixed, despite permeability varying from one kind of soil to another.

(4) The runoff contributions from saturated and unsaturated land are respectively examined through calculating the two rhs terms in (12) with the stochastic analogue–yielded data. Results show that their values are in quite good concord with the theoretical results of subsection 4.1 (figure not shown). For instance, higher rainfall intensity over a small area (small α) makes small contribution to the whole area. Especially, for a smaller $E(S)$, much runoff over the whole grid region is actually from unsaturated land.

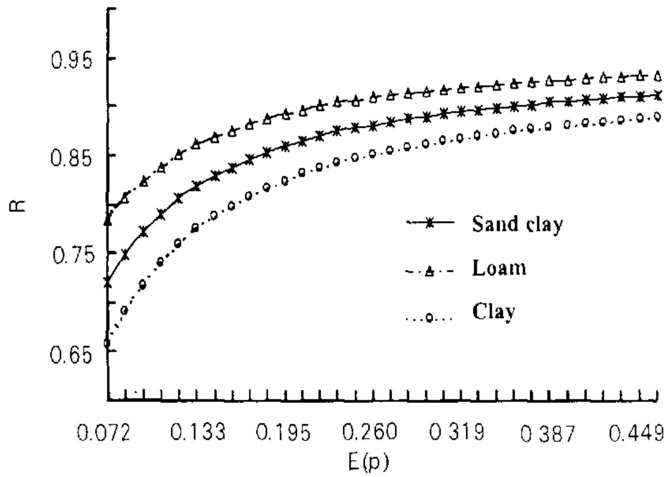

Fig. 7. Variations of runoff ratio with $E(P)$.

5. Summary

Starting from the physical mechanism of land surface hydrological processes in conjunction with statistical distribution theory, a analytical expression for runoff ratio is derived for subgrid–scale inhomogeneous land generated through heterogeneous soil moisture distribution and precipitation, thus simplifying the parameterization which is the so–called mosaic scheme. The unique merit of this expression for runoff ratio is that a sensitivity experiment can be undertaken by means of a few parameters for describing heterogeneous land either in on–line or off–line state. Clearly, it favors, to great extent, the real time operation of air–land coupling models.

From the theoretical expressions, the intricate mechanism of land surface hydrology (e.g., runoff) can normally be presented in terms of integral components for flux contribution under the stress of top–layer saturated and unsaturated areas (similarly, intense and weak rainbelts). Hence, the calculation of grid area mean fluxes can be converted into the integration of weighted fluxes in subregions with dissimilar soil properties. This subgrid treatment can be extended to the estimation and simulation of the exchange of various kinds of fluxes.

Experiments on the feasibility and sensitivity of the expression yield some useful conclusions. 1) If the $E(P)$ is fixed, the runoff ratio is relatively low on the land surfaces with higher permeability (such as sand). 2) The wetted soil surface (higher $E(s)$) has bigger contribution to surface runoff in the whole region regardless of the value of λ and α. 3) The runoff ratio R varies with soil properties, with the maximum R in clay, minimum in sand soil and moderate in loam's analog soil. The runoff ratio from theoretical calculation agrees well with the mosaic regional mean runoff ratios with relative errors of 6.0%–7.0%, on the average. 4) With the increase of area mean moisture, the runoff ratio is enhanced for all kinds of soil. That is, with the same rainfall intensity, R intensifies as regionally averaged soil humidity is reinforced although permeability differs from soil to soil. 5) The regional mean surface runoff is mainly affected by the heterogeneous soil–water distribution and uneven rainfall distribution.

REFERENCES

Allen, D. M., C. T. Haan et al., 1975: Stochastic simulation of daily rainfall, Res. REP., **82**, 2–21

Avissar, R., 1992. Conceptual aspects of a statistical-dynamic approach to represent landscape subgrid-scale heterogeneities in atmospheric models. *J. Geophys. Res.*, **97**, 2729–2742.

Avissar, R., 1993: Observations of leaf stomatal conductance at the canopy scale: An atmospheric modeling perspective. *Bound. -Layer Meteor.*, **64**, 127–148.

Clapp, R. B., and G. M. Hornberger, 1978. Empirical equations for some soil hydraulic properties. *Water Resour. Res.*, **117**(1), 311–314.

Dikinson, R. E., P. J. Kennedy et al., 1986: Biosphere–Atmosphere Transfer Scheme (BATS) for the NCAR community climate model, NCAR Tech. Note, NCAR / TN-275+STR. 69pp.

Ding Yuguo, and Zhang Yaocun, 1989: Stochastic modeling experiments on precipitation's climate characteristics. *J Nanjing Inst. Meteor.*, **12**(2), 19–29 (in Chinese).

Ding Yuguo, 1987: An indirect model for probability distribution of rainfall. *ibid.* **10**(4), 407–415 (in Chinese).

Ding Yuguo, 1994: Study on universality of precipitation distribution models. *Scientia Atmospherica Sinica*, **18**(5), 552–560 (in Chinese).

Eagleson, P. S., 1984: The distribution of catchment coverage by stationary rainstoms. *Water Resour Res.*, **20**(5), 581–890.

Eagleson, P. S., and Q. Wang, 1985: Moments of catchment storm area. *Water Resour. Res.*, **21**(8), 1185–1194.

Eagleson, P. S., N. M. Fennessey, Q. Wang, and I. Rodriguez-Iturbe, 1987: Application of spatial Possisson models to air mass thunderstorm rainfall. *J. Geophys. Res.*, **92**(D8), 9661–9678.

Entekhabi, D., and P. S. Eagleson, 1989: Land surface hydrology parameterization for AGCM including subgrid scale spatial variability. *J. Climate*, **2**, 816–830.

Giorgi, P., 1997: Approach for the representation of surface heterogeneity in land surface models Part I: Theoretical framework. *Mon. Wea. Rev.*, **125**, 1885–1899.

Larsen, G. A., and R. B. Pense., 1982: Stochastic simulation of daily climate data for agronomic models. *Agr. J.*, **74**, 510–514.

Ma Ainai, 1998: *Remote Sensing Information Models*. Peking University Press, 45–60 (in Chinese).

Olkin, I., L. T. J. Gleser, and C. Derman, 1980: *Probability Models and Applications*, Macmillan Publishing Co., Inc., printed in U. S. A, 262–274.

Pielke, R. A., 1990: *Modelings of Meso-Scale Meteorology*, translated by Zhang Xingzhen and Yang Changxin, China Meteorological Press, Beijing, pp. 425–426 (in Chinese).

Sellers, P. J., Y. Mintz, Y. C. Sud, and A. Delcher, 1986: A Simple Biosphere Model (SiB) for use with general circulation models, *J. Atmos. Sci.*, **43**, 505–531.

Tian Guoliang, 1991. Techniques for Telemetrically monitoring soil water. *Environmental Remote Sensing*, **6**(2), 89–98.

Warrilow, D. A., A. B. Sangster, and A. Slingo, 1986: *Modeling of Land Surface Processes and Their Influence on European Climate*, U. K. Meteor. Office, DCTN, 38, 94pp.

Xiao Qianguang, Chen Weiying, Sheng Yongwei et al., 1994: Experimental research of weather satellite monitoring soil moisture. *J. Appl. Meteor.*, **5**(3), 312–318.

Xue, Y. K., P. J. Sellers, J. L. Kinter, and J. Shukla, 1991: A simplified biosphere (?) model for global climate studies, *J. Climate*, **4**, 345–364.

Yu Tao, and Tian Guoliang, 1997: The use of thermal inertia in the monitoring of variations in top-layer soil moisture. *J. Remote Sensing*, **1**(1), 24–31.

Zhang Xuewen, and Ma Li, 1992: *Entropy of Meteorology*, China Meteorological Press, Beijing, pp. 53–158 (in Chinese).

Zhang Xuewen, 1987: Laws of specific humidity distribution in the atmosphere. *ibid*, **45**(3), 251–253 (in Chinese)

Zhang Zhenqiu, and Li Weiliang, 1998: Entropy theory and parameterization of nonuniform distribution of precipitation. *Acta Meteorologica Sinica*, **12**(3), 334–344.

Zhou Guoyi, 1997: *Principles of Ecosystem's Moisture and Heat with Applications*. China Meteorological Press, Beijing, 118–127 (in Chinese).

非均匀地表条件下区域平均径流率的一种参数化方法及其模拟试验

刘晶淼　　丁裕国　　周秀骥　　王纪军

摘　要

从陆面水文过程的物理机制出发，引进概率统计分布理论，推导出一种由非均匀土壤含水量及降水气候强迫所形成的次网格尺度非均匀径流率的解析表达式，从而将通常的次网格尺度地表径流的参数化方案(mosaic 方法)改进为考虑网格区整体非均匀性的统计–动力参数化方案。文中用仿真模拟资料验证了该方案的可靠性与可行性，并作数值试验。结果表明，该方案切实可行。

关键词：陆面过程，水文学，次网格尺度，非均匀性分布，概率分布密度